CHAPTER FIVE

Detection of DNA by Sequence-Specific Intercalation

The text of this chapter was taken in part from a manuscript co-authored with Bogdan Olenyuk and Professor Peter B. Dervan (Caltech).

Fechter EJ, Olenyuk B, Dervan PB; Sequence-Specific Fluorescence Detection of DNA by Polyamide-Thiazole Orange Conjugates, **2005**, *In preparation.*

Abstract

Highly sensitive fluorescent methods to detect specific double-stranded nucleic acid sequences may be useful in the field of genetics. Three pyrrole-imidazole polyamides were conjugated to thiazole orange at the C- termini and their fluorescence properties examined in the presence and absence of match duplex DNA. The conjugates fluoresced weakly in the absence of DNA but showed significant enhancement (>1000 fold) upon the addition of one equivalent match DNA and only slight enhancement with the addition of mismatch DNA. The compounds bound specific DNA sequences with high affinity and selectivity and unwind the DNA duplex through intercalation. The polyamide-thiazole orange conjugates were also capable of localizing in the nucleus of certain cell lines, signifying their potential applications in live cells. This new class of polyamides provides an extremely sensitive method to specifically detect DNA sequences without denaturation.

Introduction

Efforts to understand gene arrangements and their cellular functions have led to an increased interest in the rapid detection of specific nucleic acid sequences.[1-3] Traditional approaches involve homogeneous hybridization assays, which typically use single-stranded oligonucleotide probes to generate fluorescent signal amplification upon hybridization at their designed complementary match sites.[1-7] Examples include the molecular beacons, in which a fluorophore and quencher are conjugated to a DNA hairpin at the 5' and 3' ends, respectively.[1-3] Fluorescence emission is detected upon probe hybridization to its target single stranded DNA site by separating the fluorophore from the quencher. Another class, the "light-up probes," utilize a peptide nucleic acid (PNA) conjugated to a thiazole orange (TO) cyanine dye.[7] The PNA directs the conjugate to a specific hybridization site where emission of the relatively non-fluorescent dye is enhanced by approximately 50-fold. In both cases signal enhancement is only reported upon hybridization to single-stranded DNA, thus requiring denaturation conditions for the detection of a DNA duplex. A series of peptide-thiazole orange conjugates was also recently shown to have excellent fluorescence enhancement properties upon binding to calf thymus (CT) DNA but were not shown to have sufficient DNA sequence specificity.[8]

Pyrrole-imidazole polyamides are a class of minor groove-binding ligands that can be programmed to recognize specific DNA sequences with affinities and specificities comparable to DNA binding proteins.[9] Our lab showed that polyamides with tetramethyl rhodamine (TMR) tethered to an internal pyrrole ring display modest sequence-specific fluorescence enhancement (≥10-fold) upon binding to match duplex DNA.[10] Although these conjugates bound DNA with slightly reduced affinity relative to their parent compounds

(those not containing TMR), the detection method proved useful in probing the interactions between polyamides and non-Watson-Crick DNA base pairs. Our group also demonstrated that covalently linking acridine to a hairpin polyamide permits both intercalation and groove binding while retaining the polyamide's capacity for sequence discrimination (see Chapter two).[11,12] These polyamide-intercalator conjugates were utilized to inhibit the binding of the major groove binding transcription factor GCN4, presumably by helix distortion. Utilizing the programmable nature of a minor groove-binding polyamide combined with a fluorophore that enhances only upon intercalation may provide a highly specific and sensitive method for the detection of duplex DNA (Figure 5.1).

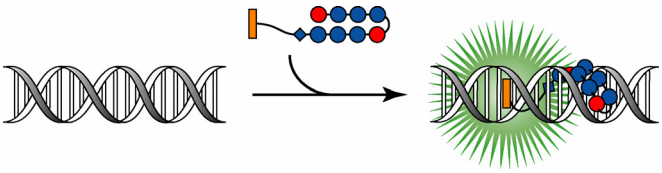

Figure 5.1 Fluorescence detection model. A polyamide-fluorophore conjugate shows fluorescent enhancement upon binding its match site of DNA.

Thiazole orange is a prototypical member of the class of dyes known as cyanines, which show fluorescent enhancements from 200- to 3,000-fold when intercalatively bound to DNA.[13-16] The dyes are believed to freely rotate in solution permitting radiational energy loss but, upon binding through intercalation, the conformational restriction of rotation can enforce a planar resonance structure and allow fluorescence emission (Figure 5.2).[13-16] The dye's structure also can be modified to tune its absorption and emission profiles,[17] which may be useful with fluorescence resonance energy transfer (FRET) experiments or when used in the presence of other fluorophores. Moreover, the linker length can easily be modified to suit any number of applications.

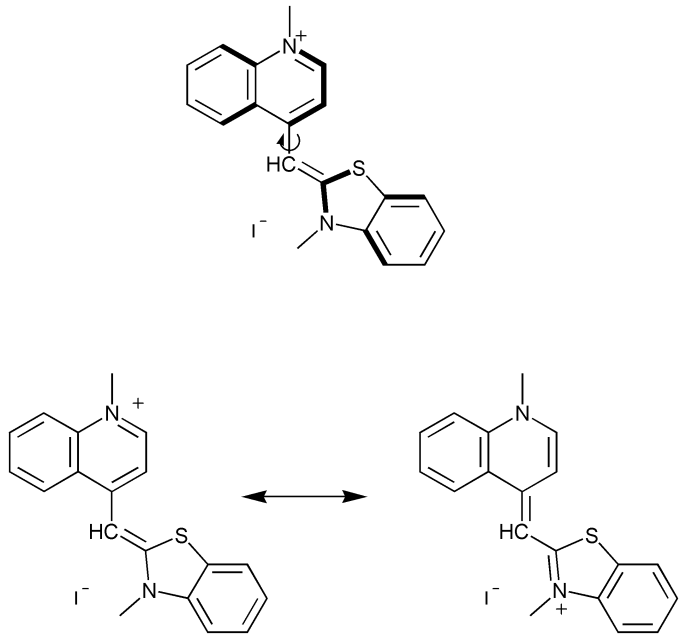

Figure 5.2 Thiazole orange fluorescence enhancement model. The chromophore is free to rotate in solution (top) leading to radiative loss of energy. Upon binding DNA the chromophore becomes planarized to allow resonance and fluorescence enhancement.

We report here the synthesis and fluorescence properties of three polyamide-TO conjugate probes and their abilities to detect specific sequences of double helical DNA in homogeneous solution (Figures 5.3 and 5.4). The polyamide provides a sequence-specific scaffold to deliver a TO intercalator to a predetermined DNA site. Solution-structure data of a thiazole orange dimer (TOTO)[18] show the linker attachment to the TO at the minor groove-residing quinoline nitrogen. Based on previous polyamide-intercalator designs[11,12] and the structure data of TOTO, the polyamide C-terminus was linked to the quinoline nitrogen using polyethylene glycol (PEG). The conjugates bind specifically to target match site double helical DNA *without* reduced affinities and unwind closed circular DNA (ccDNA), supporting the intercalation model of thiazole orange within this construct. The conjugate probes are relatively non-fluorescent in the absence of DNA and display a substantial increase in fluorescence (>1000 fold) upon addition of DNA containing a target match site.

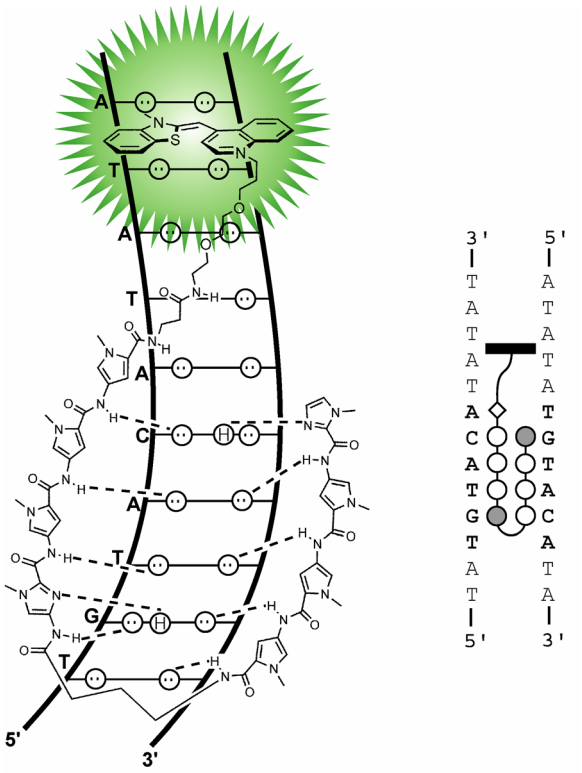

Figure 5.3 DNA binding model for the eight-ring hairpin polyamide conjugate ImPyPyPy-γ-PyPyPyIm-β-PEG_2-TO bound to the minor groove of 5'-TGTACAT-3'. (Left) Circles with dots represent lone pairs of N3 of purines and O2 of pyrimidines. Circles containing an H represent the N2 hydrogens of guanine. Putative hydrogen bonds are illustrated by dotted lines. (Right) Solid circles represent imidazoles (Im), open circles represent pyrroles (Py), and diamonds denote β-alanine (β). The shaded bar depicts the thiazole orange intercalator. Fluorescence emission from the conjugate-DNA complex is represented in green. According to the pairing rules, Im/Py codes for G•C, Py/Py for A•T or T•A, Py/Im for C•G, and β-alanine for A.T.

Results and Discussion

Synthesis of Polyamide-Thiazole Orange Conjugates

Synthesis of the thiazole orange PEG-linked precursor **6** (TO-PEG) is shown in Figure 5.5 and described in the experimental section. Resin-bound eight-ring hairpin

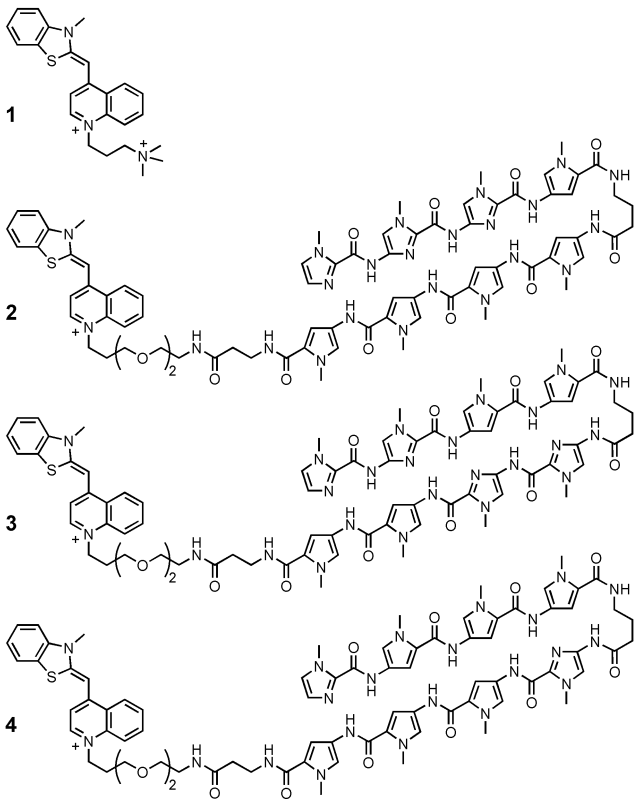

Figure 5.4 Structures TO-PRO-1 **1** and hairpin polyamide-TO conjugates **2**-**4**.

polyamides were synthesized in a stepwise manner on Boc-β-alanine Phenyl-acetamido-methyl (PAM) resin according to established Boc-chemistry protocols (Figure 5.6).[19] The carboxylate containing polyamides **5a**-**5c** were cleaved from PAM resin through overnight treatment with LiOH in methanol. Following purification, the polyamide carboxylate was coupled to the free amine of TO-PEG **6** with diphenylphosphoryl azide (DPPA) and TEA in DMSO for 2hr. Crude conjugates **2**-**4** were each purified by preparatory reverse phase HPLC and stored as dry aliquots at -80°C.

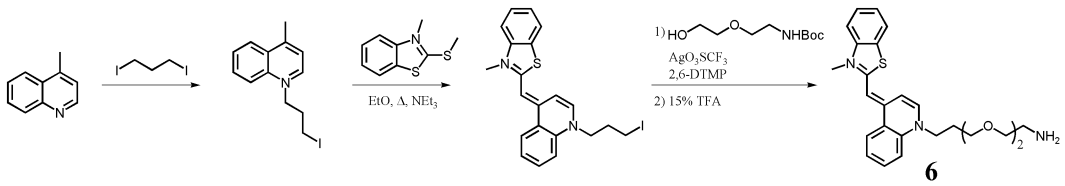

Figure 5.5 Sythesis of thiazole orange PEG precursor **6**.

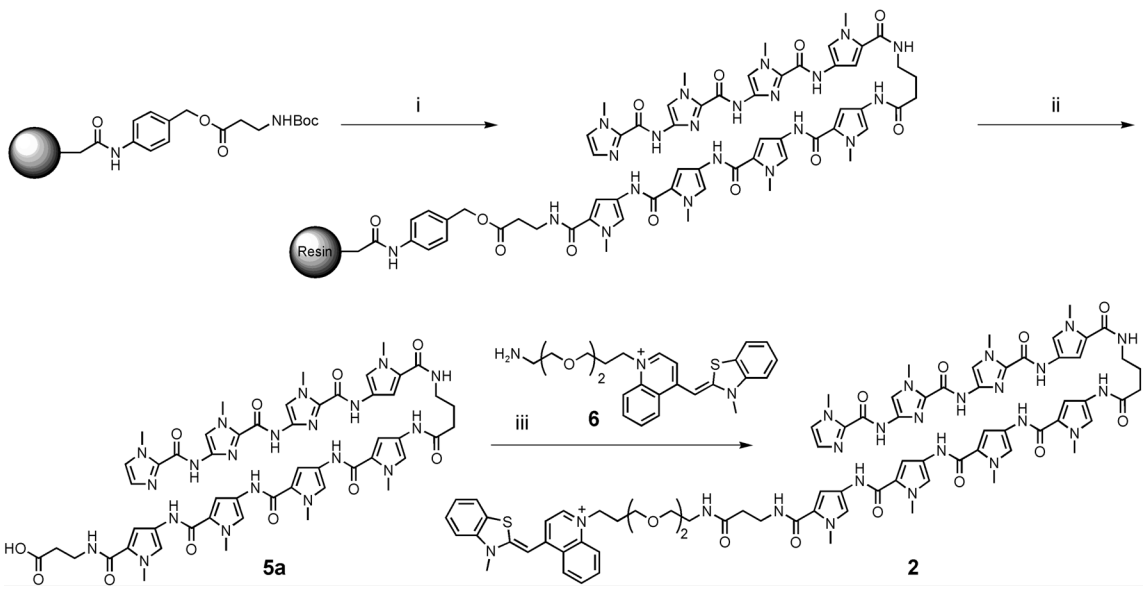

Figure 5.6 Synthesis of polyamide-TO conjugates. (i) Solid-phase Boc chemistry[19] (ii) 1M LiOH, MeOH, THF, 37 °C (iii) **5a**, DPPA, TEA, DMSO, 2 h.

Binding Energetics and Sequence Specificity

DNA-binding properties of **2**-**4** were investigated by quantitative DNase I footprinting titration assays (Figure 5.7).[20] The 5'-^{32}P-labeled PCR-amplified fragment of pEF15 (Figure 5.7a) contains one match site for each of the three polyamide-TO conjugates. The equilibrium association constants (K_a) at their target match sites are 3 x 10^8 M^{-1}, 4 x 10^9 M^{-1}, and 1 x 10^{10} M^{-1}, for **2**, **3**, and **4**, respectively. By comparison, the parent polyamides of **2**-**4** (those containing N,N-dimethylaminopropylamine in lieu of **6** at the C-terminus) bound DNA with approximately the same affinities (4 x 10^8 M^{-1}, 4 x 10^9 M^{-1}, and 2 x 10^{10} M^{-1}, respectively).[21-23] Because polyamides conjugated to non-intercalating moieties (such as fluorescent dyes and peptides) generally display decreased binding affinities relative to their parent polyamides, it appears that the conjugated TO moiety contributes to the DNA binding affinity. Additionally, tethering TO to these polyamides does not diminish their

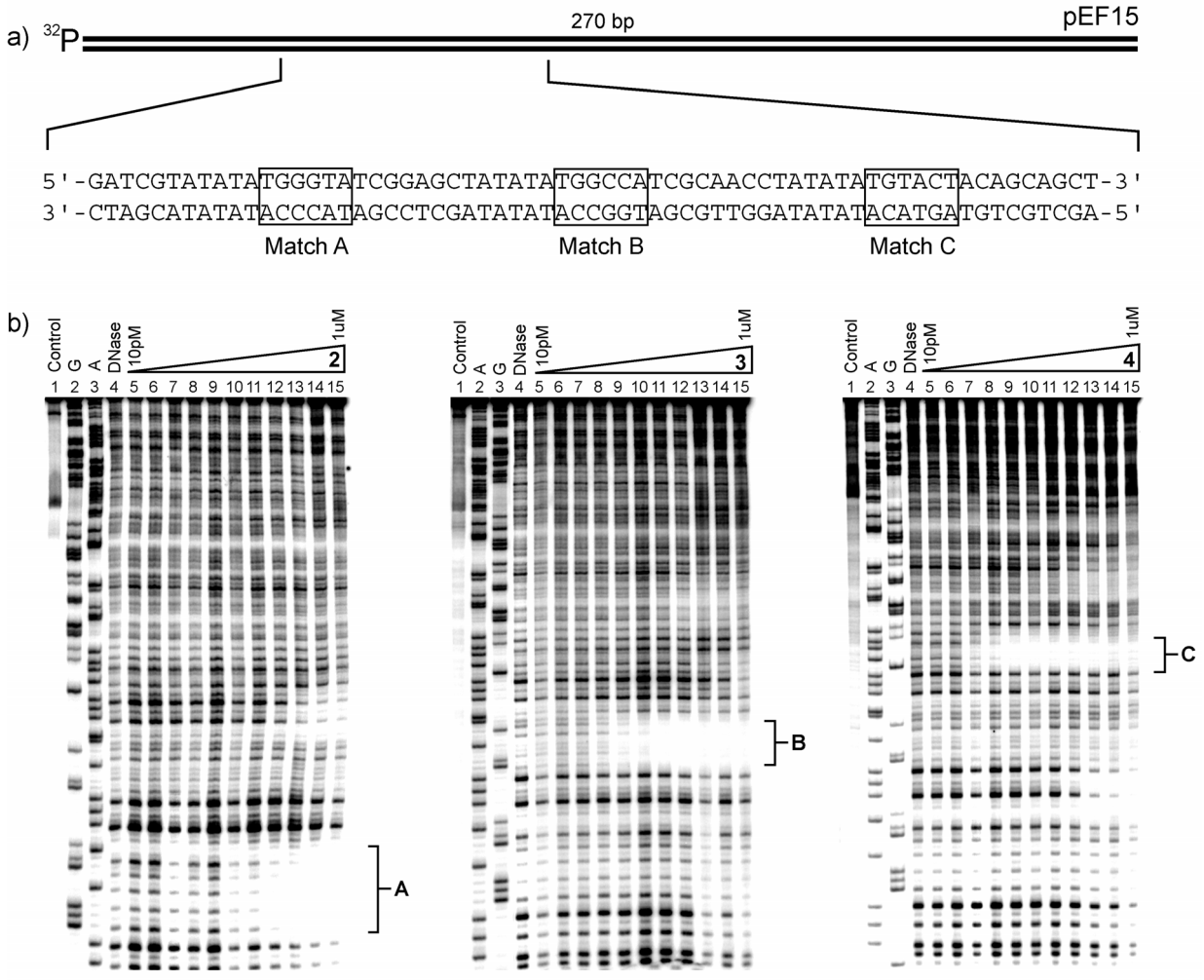

Figure 5.7 (a) Sequence of the synthesized insert from the pEF15 plasmid containing the boxed 7-bp target sites Match A, Match B, and Match C for conjugates **2**, **3**, and **4**, respectively. (b) Quantitative DNase I footprint titration experiments with conjugates **2** (left), **3** (middle), and **4** (right) on the PCR-amplified 5'-^{32}P-labeled fragment from pEF15. Lane 1, intact DNA; lanes 2 and 3, sequencing reactions; lane 4, DNase I standard; lanes 5-15, DNase I digestion products in the presence of 10, 30, 100, and 300 pM; 1, 3, 10, 30, 100, and 300 nM; and 1 μM polyamide, respectively.

sequence specificities, as compounds **2-4** display no detectable binding outside of their targeted match sites (Figure 5.7b).

Helical Unwinding Angle Determination

The DNA-unwinding properties of TO-PRO-1 **1** and polyamide-TO **3** were determined from a helical unwinding assay, developed by Crothers and Zeman, capable of providing an unwinding angle (ϕ) from sequence-specific interactions.[24-25] A series of

relaxation reactions were carried out using topoisomerase I (Topo I) on closed-circular pUC19 DNA pre-equilibrated with varying concentrations of polyamides. Plasmids were extracted from the polyamide conjugates with phenol-chloroform and separated by two dimensional (2D) agarose gel electrophoresis to differentiate the resulting distribution of topoisomers. Increased DNA unwinding shifts the final topoisomer distribution toward a more negatively supercoiled population. Each reaction containing dye **1** or conjugate **3** resulted in a negative distribution of topoisomers, whereas control experiments lacking added intercalators resulted in a primarily positive distribution of topoisomers. Mathematical analysis of the topoisomer distributions showed decreasing apparent unwinding angles (ϕ_{ap}) for simultaneously decreasing conjugate and plasmid concentrations (Figure 5.8). The actual average unwinding angles (ϕ) for binding to pUC19 were determined from the ordinate intercepts. TO-PRO-1 **1** unwinds DNA ~17° whereas polyamide-TO conjugate **3** unwinds pUC19 an average of ~8° per binding event. The decreased propensity of unwinding by **3** is not surprising since slight linker modifications have been shown to significantly alter the binding properties of TO derivatives.[26,27] It's also noteworthy that the negative inverses of the slopes from this assay are proportional to the average binding affinities for each dye to pUC19. In accord with the higher affinity of conjugate **3** found by DNase I footprinting, the

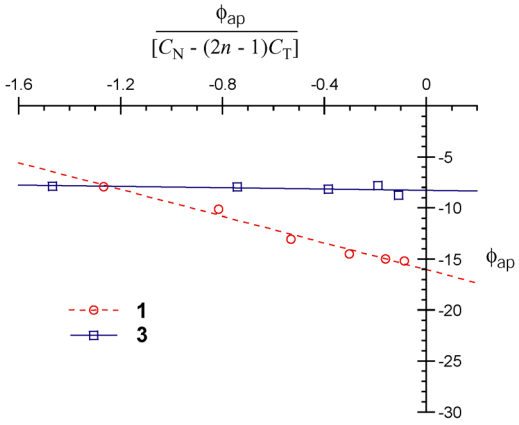

Figure 5.8 Unwinding plots for TO-Pro-1 **1** and polyamide-TO conjugate **3** on pUC19. Each data point was calculated from one set of topoisomer distributions from reactions containing polyamide compared to a control distribution lacking polyamide. Interception of the ordinate yields the unwinding angle (ϕ) per polyamide-TO conjugate.

slope shown for **3** is less negative than the slope of **1**. The evidence of intercalation and high binding affinity of **3** suggests polyamide-TO conjugates are likely good candidates for fluorescence enhancement upon DNA binding.

Detection of Specific Double-Stranded DNA Sequences

The fluorescence properties of polyamide-TO conjugates **2**-**4** were examined in the presence and absence of three different hairpin-forming DNA oligomers (Figure 5.9). Each synthetic 37-mer was designed with a match site for one of three polyamide-TO conjugates (**2**, **3**, and **4** are programmed to bind Oligo A, Oligo B, and Oligo C, respectively). Figure 5.10a shows the absorption spectra of TO-PRO-1 (**1**), unconjugated polyamide (**5b**), and polyamide conjugated to thiazole orange (**3**) free in solution at room temperature. The polyamide-TO absorption is slightly red-shifted (~6 nm) with a somewhat decreased molar absorptivity relative to the TO-Pro-1 fluorophore alone. The fluorescence of 100 nM solutions of polyamide-TO conjugates in aqueous solution (1x TKMC) without DNA is almost negligible – indicative of free rotation between the benzothiazole and quinoline rings as well as minimal back-bonding of the fluorophore to the polyamide core.[28] Addition of match DNA to the conjugates increases their fluorescence intensities (Figure 5.10b). Fluorescence enhancements of all three conjugates in the presence of their match oligomers are ~1000-fold at 1:1 DNA-polyamide stoichiometry.

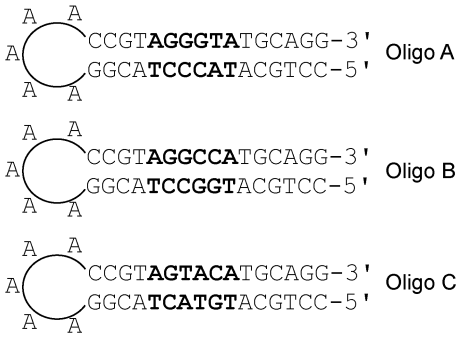

Figure 5.9 Design of hairpin-forming duplex oligonucleotides Oligo A, Oligo B, and Oligo C containing match sites (shown in bold) for polymides **2**, **3**, and **4**, respectively.

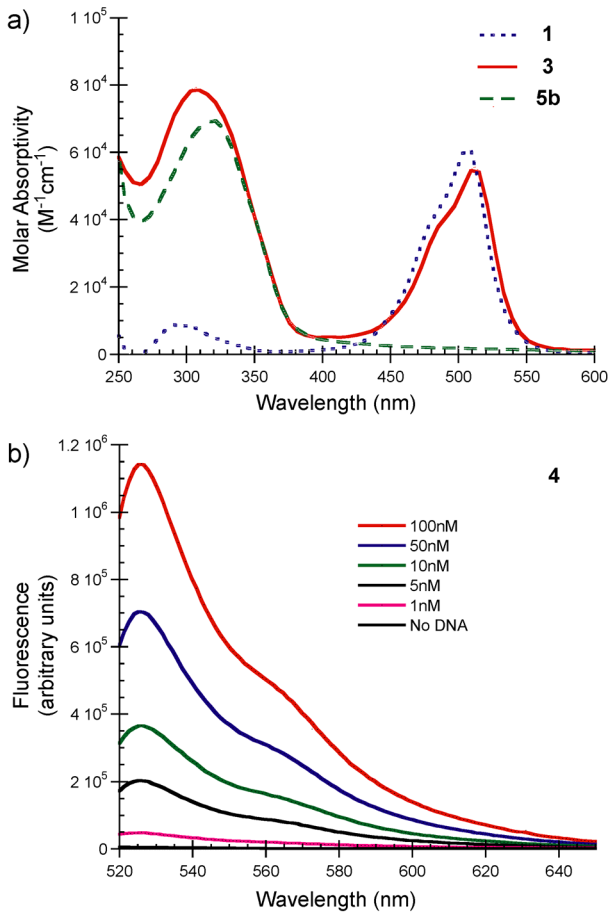

Figure 5.10 (a) Absorption spectra of free polyamide-TO conjugate **3** (—), free unconjugated polyamide **5b** (– –), and free TO-Pro-1 **1** (····). (b) Fluorescence emission profile for polyamide-TO conjugate **4** at 100 nM concentration in the presence of increasing concentrations of Oligo C (1 nM-100 nM).

The ability of each conjugate **2-4** to distinguish its match site from non-match DNA was examined by direct laser excitation scanning through the bottom of polystyrene plates. The emission data for polyamide-TO conjugates in the presence of each hairpin oligomer at 1:1 DNA:polyamide stoichiometry and 100 nM is presented in Figure 5.11. The increased fluorescence enhancement of each conjugate when bound to its corresponding match DNA oligomer relative to mismatch and control mixtures can be seen visually in Figure 5.11a. Normalized fluorescence data for conjugates bound to each oligomer is shown in Figure 5.11b. The four-imidazole containing conjugate **3** has the highest selectivity for fluorescence

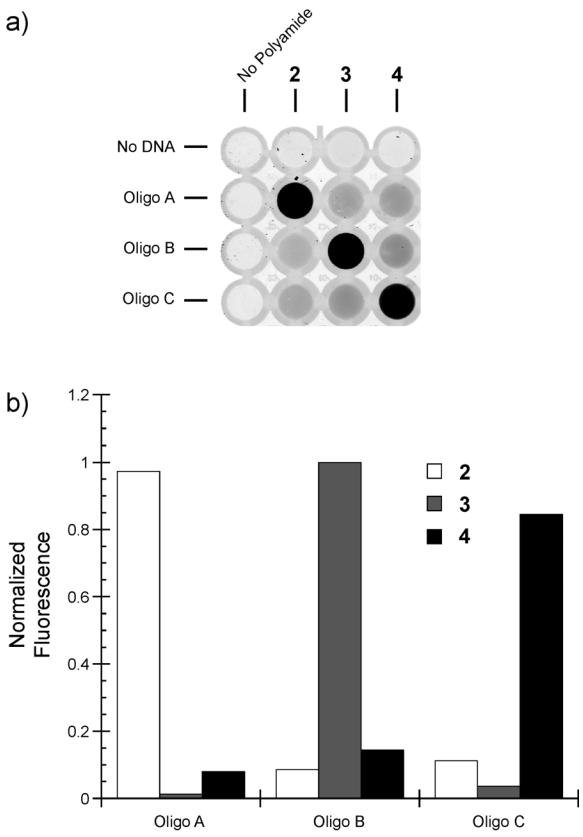

Figure 5.11 (a) Plate experiment conducted at 100 nM polyamide-TO in the presence of 100 nM of three different oligonucleotides. Each conjugate preferentially binds and shows fluorescent enhancement at the designed DNA match site. The fluorescence intensity correlates with the darkness of the well. (b) Normalized data for the plate experiment using the buffer well as the background fluorescence. The fluorescence intensities of the polyamides without DNA is at least 1000-fold lower than the maximum intensities and are not shown on the bar graph above.

emission, with virtually no enhancement in the presence of mismatch Oligo A or Oligo B. Conjugates **2** and **4** (containing three and two imidazole amino acids, respectively) showed only slightly decreased specificities by fluorescence. Polyamides typically have higher specificity with increased imidazole content,[9] which may account for the different specificities of **2**-**4** in the presence of the nanomolar concentrations of DNA required for these experiments. Nonetheless, with each oligomer the fluorescence enhancement is relatively small for conjugates not programmed to bind the sequence and drastically increased for the conjugate containing the appropriate pyrrole-imidazole arrangement.

These data support a model where the polyamide moiety directs the non-fluorescent conjugate to a specific site of the DNA duplex and delivers the tethered thiazole orange fluorophore to an adjacent site. Upon polyamide binding, the thiazole orange likely intercalates the DNA and the conformation of the normally free rotating fluorophore is restricted, resulting in substantial fluorescence emission following excitation.

Cellular Localization

Identifying unique DNA sequences within a living cell would be an exciting application of polyamide-thiazole orange conjugates. The potential use in a cellular environment is dependent on the ability of the conjugates to reach the nucleus.[29,30] The intracellular distribution of all three conjugates in several cell lines were determined by confocal laser scanning microscopy (Table 5.1). It appears the conjugates are not nuclear in many cell lines. However, in MCF-7, HeLa, SK-BR-3, Jurkat, and CEM cell lines the conjugates are nuclear. Interestingly, several images show the conjugates localizing as speckles within the nucleus or regions of the cytoplasm (Figure 5.12). Also, many of the indicated cell lines that did not permit nuclear uptake instead show the conjugates as localizing in the mitochondria. Since the conjugates should fluoresce only when tightly associated with another object, the actual cellular distribution may be difficult to identify.

Table 5.1 Cellular localization data for polyamide-thiazole orange conjugates in tested cell lines*.

polyamide	MCF-7	HeLa	PCL3	LN-CaP	SK-BR-3	DLD-1	786-O	293	Jurkat	CEM	MEG-01	MEL	NB4	3T3
2	+	+	-	--	+	--	--	-	+	+	c	c	c	--
3	--	--	-	--	+	--	--	-	-	+	c	c	c	--
4	+	+	--	--	+	--	-	--	+	+	--	-	+	+

* + +, Nuclear staining exceeds that of the medium; +, nuclear staining less than or equal to that of the medium but still prominent; -, very little nuclear staining with the most fluorescence seen in the cytoplasm and/or medium; --, no nuclear staining; c, cytoplasmic.

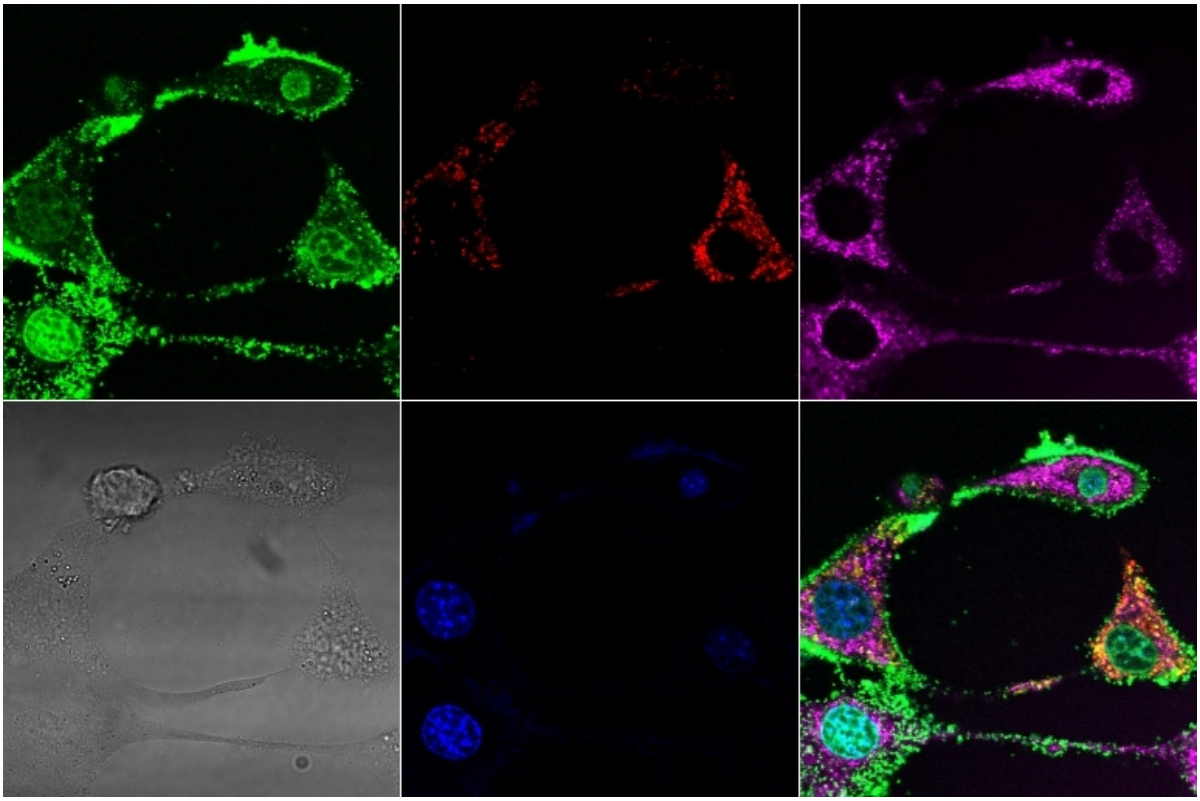

Figure 5.12 Cellular localization of polyamide-thiazole orange conjugates in 3t3 cell line. *Top row* (left to right): polyamide-TO **4**, Mito Tracker, Lyso Tracker. *Bottom row* (left to right): visible light image, Hoechst, overlay.

Polyamide-TO conjugates represent a new class of DNA-binding agents that detect specific sequences of double-stranded DNA. The conjugates 1) bind specifically and with high affinity to target match site double-helical DNA, 2) unwind DNA, presumably by intercalation, and 3) localize in the nucleus of some cell lines. Importantly, the generally non-fluorescent conjugates show significant fluorescent enhancement only upon excitation in the presence of DNA containing the match site tested. These conjugates show promise as probes for biologically important sequences such as triplet repeats and transposable elements, as well as chromosome paints for telomeric and centromeric repeats.

Experimental

Materials

TO-PRO-1 (**1**) was purchased from Molecular Probes. Lepidine (4-methylquinoline) and 3-methyl-2-(methylthid)benzothizolium p-toluenesulfonate were purchased from Aldrich. Restriction endonucleases were purchased from New England Biolabs and used as noted in the manufacturer's protocol. [γ-^{32}P]-Adenosine-5'-triphosphate (≥6000 Ci/mmol) was obtained from ICN. Purified pUC19 DNA for unwinding angle determination was isolated from transformed JM109 *Escherichia coli* using the Qiagen protocol. EDTA, dithiothreitol (DTT), ultrapure agarose, and calf thymus Topo I were purchased from Gibco/BRL. Micron 50 microconcentrators were purchased from Amicon. Micro Columns were purchased from Amersham Pharmacia Biotech, Inc. Water (18 MΩ) was obtained from a Millipore MilliQ water purification system, and all buffers were 0.2 μm filtered. Polystyrene plates (#62409-068) were from VWR Scientific. Reagent-grade chemicals were used as received unless otherwise stated.

UV spectra were measured in water on a Beckman model DU 7400 diode array spectrophotometer. Fluorescence spectrophotometer measurements were obtained at room temperature on an ISS K2 spectrophotometer employing 5 nm emission and excitation slits in conjunction with a Hg lamp. TO fluorescence was measured in polystyrene plate on a Molecular Dynamics Typhoon, employing a 532 nm excitation laser and a 526-nm short-pass emission filter. HPLC analysis was performed on a Beckman Gold system using a RAININ C_{18}, Microsorb MV, 5 μm, 300 x 4.6 mm reversed-phased column in 0.1% (v/v) TFA with acetonitrile as eluent and a flow rate of 1.0 mL/min. Preparatory reversed-phase HPLC was performed on a Beckman HPLC using a Waters DeltaPak 25 x 100 mm, 100 μm C_{18} column

equipped with a guard, 0.1% (wt/v) TFA, 0.25% acetonitrile/min. Matrix-assisted laser desorption/ionization time-of-flight mass spectrophotometry (MALDI-TOF) was performed using an Applied Biosystems Voyager DE-Pro.

ImImImPy-γ-PyPyPyPy-β-PEG$_2$-TO (2)

Compound **5a** (1 μmol aliquot) was dissolved in 500 μL DMSO and treated with **6** (3.5 μmol), diphenylphosphoryl azide (DPPA, 5 μL), TEA (20 μL), and stirred at room temperature for 2 h. The mixture was diluted with 0.1% (w/v) TFA (8 mL) and DMF (2 mL), and the resulting solution was purified by reversed-phase HPLC. Lyophilization provided ImImImPy-γ-PyPyPyPy-β-PEG$_2$-TO (**2**) as a red powder (0.65 mg, 42% recovery). MALDI-TOF-MS (monoisotopic) calcd for $C_{77}H_{86}N_{23}O_{12}S$ (M+H): 1557.7. Found: 1557.7.

ImImPyPy-γ-ImImPyPy-β-PEG$_2$-TO (3)

Synthesized as described for **2** starting from 1 μmol **5b** (0.75 mg, 48% recovery). MALDI-TOF-MS (monoisotopic) calcd for $C_{76}H_{85}N_{24}O_{12}S$ (M+H): 1558.7. Found: 1558.9.

ImPyPyPy-γ-ImPyPyPyPy-β-PEG$_2$-TO (4)

Synthesized as described for **2** starting from 1 μmol **5c** (0.69 mg, 44% recovery). MALDI-TOF-MS (monoisotopic) calcd for $C_{78}H_{87}N_{22}O_{12}S$ (M+H): 1556.7. Found: 1557.0.

ImImImPy-γ-PyPyPyPy-β-OH (5a)

A sample of ImImImPy-γ-PyPyPyPy-β-resin (200 mg, 0.38 mmol/g) was suspended in 6 mL THF, 1.5 mL methanol, and 1.5 mL LiOH (1M) and heated at 37°C for 12 h. The reaction mixture was filtered to remove resin, concentrated *in vacuo*, and diluted with 0.1% (w/v) TFA (8 mL) and DMF (2 mL). The resulting solution was purified by reversed-phase

HPLC. Lyophilization provided ImImImPy-*γ*-PyPyPyPy-*β*-OH (**5a**) as a white powder (5.6 mg, 7% recovery). MALDI-TOF-MS (monoisotopic) calcd for $C_{52}H_{58}N_{20}O_{11}$ (M+H): 1139.5. Found: 1139.4.

ImImPyPy-*γ*-ImImPyPy-*β*-OH (5b)

Synthesized as described for **5a** using ImImPyPy-*γ*-ImImPyPy-*β*-resin (6.8 mg, 8% recovery). MALDI-TOF-MS (monoisotopic) calcd for $C_{51}H_{57}N_{21}O_{11}$ (M+H): 1140.5. Found: 1140.6.

ImPyPyPy-*γ*-ImPyPyPy-*β*-OH (5c)

Synthesized as described for **5a** using ImPyPyPy-*γ*-ImPyPyPy-*β*-resin (9.7 mg, 12% recovery). MALDI-TOF-MS (monoisotopic) calcd for $C_{53}H_{59}N_{19}O_{11}$ (M+Na): 1160.5. Found: 1160.8.

1-{3-[2-Amino-ethoxy)-ethoxy]-propyl}-4-(3-methyl-3*H*-benzothiazol-2-ylidenemethyl)-quinolinium (6)

1'-(3'-Iodopropyl)-3-methyl-oxa-4'-cyanine iodide[16,31] (200 mg, 0.340 mmol) and 2-(2-Boc-aminoethoxy)ethanol[32] (697 mg, 3.4 mmol) were dissolved in 50 mL chloroform. To this was added 2,6-Di-*tert*-butyl-4-methylpyridine (140 mg, 0.68 mmol) and AgO_3SCF_3 (175 mg, 0.68 mmol), and the reaction was stirred overnight at room temperature under Ar. The solvent was filtered and removed *in vacuo*, and the remaining residue was dissolved in 200 mL 15% TFA/DCM and allowed to stir for 4 h. The mixture was concentrated *in vacuo* and 50 mg of crude residue was dissolved in 0.1% (wt/v) TFA (8 mL) and DMF (2 mL) and purified by reversed-phase HPLC. Lyophilization provided **6** as a red powder (3.7 mg, 10%

overall recovery). 1H NMR (DMSO, TMS): δ MALDI-TOF-MS (monoisotopic) calc'd for $C_{25}H_{29}N_3O_2S$ (M+H): 436.2. Found: 436.0.

Construction of Plasmid DNA

The plasmid **pEF15** was constructed by insertion of the following hybridized inserts into the *Bam*HI/*Hind*III polycloning sites in pUC19: 5'-GATCG TATAT ATGGG TATCG GAGCT ATATA TGGCC ATCGC AACCT ATATA TGTAC TACAG C-3' and 5'-AGCTG CTGTA GTACA TATAT AGGTT GCGAT GGCCA TATAT AGCTC CGATA CCCAT ATATA C-3'. The insert was obtained by annealing complementary HindIII restriction fragments of pUC19 using T4 DNA ligase. The ligated plasmid was then used to transform JM109 subcompetent cells (Promega). Colonies were selected for α-complementation on 25 mL Luria-Bertani agar plates containing 50 mg/mL ampicillin. Cells were harvested after overnight growth at 37°C. Large scale plasmid purification was performed using WizardPlus Midi Preps from Promega. The presence of the desired insert was determined by dideoxy sequencing.

Preparation of 5'-End-Labelled Fragments

Two 21 base-pair primer oligonucleotides, 5'-GAATT CGAGC TCGGT ACCCG G-3' (forward) and 5'-TGGCA CGACA GGTTT CCCGA C-3' (reverse) were constructed for PCR amplication. The forward primer was radiolabeled using [γ-^{32}P]-dATP and polynucleotide kinase followed by purification using MicroSpin G-50 columns. The desired DNA segment was amplified as previously described.[20] The labeled fragment was loaded onto a 7% nondenaturing preparatory polyacrylamide gel (5% cross-link), and the desired

270 base-pair band was visualized by autoradiography and isolated. Chemical sequencing reactions were performed according to published protocols.[33,34]

Quantitative DNase I Footprint Titrations

All reactions were carried out in a volume of 400 μL according to published protocols.[20] Quantitation by storage phosphor autoradiography and determination of equilibrium association constants were as previously described.[20]

Unwinding Angle Determination

Relaxation reactions and numeric analyses were carried out as described.[11,24,25]

Optical Characterization

All measurements were performed in TKMC buffer [10 mM Tris-HCl (pH 7.0), 10 mM KCl, 10 mM $MgCl_2$, and 5 mM $CaCl_2$]. The concentration of polyamide-TO conjugate was 100 nM and the volume of solution used was 500 μL. In a fluorimeter, polyamides **2**-**4** were excited at 490 nm and measured over the interval of 520 nm to 650 nm. 100 nM solution of each conjugate was irradiated in the presence of increasing concentration of the appropriate match DNA (up to 100 nM) to generate the fluorescence enhancements reported. Absorption spectra were recorded under the same conditions as emission at higher concentrations.

Plate Characterization

In the dark, 100 μL solutions were made by titrating together a fixed concentration of 100 nM conjugate against 100 nM of each DNA oligo A-C. The solutions were gently swirled and then allowed to sit for 6 h before measurements were made. No changes in

fluorescence intensity were observed for longer equilibration times. Plates containing **2-4** were excited at 532 nm and data were collected with a 526-short pass filter. ImageQuant software (Molecular Dynamics) was used to analyze the fluorescence intensity of each experiment. The normalized data were calculated by using the relation $(F_{obs} - F_{min})/(F_{max} - F_{min})$, where F_{obs} is the sample fluorescence and F_{max} and F_{min} are the maximum and minimum fluorescence intensity, respectively.

Confocal Microscopy

All cellular uptake experiments were completed by Benjamin S. Edelson as published.[29,30] Briefly, adherent cell lines were trypsinized for 5–10 min at 37°C, centrifuged for 5 min at 5°C at 2,000 rpm in a Beckman-Coulter Allegra 6R centrifuge, and resuspended in fresh medium to a concentration of 1.25 x 10^6 cells per mL. Suspended cell lines were centrifuged and resuspended in fresh medium to the same concentration. Incubations were performed by adding 150 µl of cells into culture dishes equipped with glass bottoms for direct imaging (MatTek, Loveland, OH). Adherent cells were grown in the glass-bottom culture dishes for 24 h. The medium was then removed and replaced with 142.5 µl of fresh medium. Then 7.5 µl of the 100 µM polyamide solution was added and the cells were incubated in a 5% CO_2 atmosphere at 37°C for 10–14 h. Suspended cell line samples were prepared in a similar fashion, omitting trypsinization. These samples were then incubated as above for 10–14 h. Imaging was performed with a x40 oil-immersion objective lens on a Zeiss LSM 510 META NLO laser scanning microscope with a Coherent Chameleon 2-photon laser or on a Zeiss LSM 5 Pascal inverted laser scanning microscope.

Acknowledgment

We are grateful to the National Institutes of Health (GM-27681) for research support, a Research Service Award to E.J.F., and a postdoctoral fellowship to B.O. (F32 GM-19788).

References

1. Tyagi, S. and F. R. Kramer, *Nat. Biotechnol.* **1996**, *14*, 303-308.
2. Tyagi, S., D. P. Bratu, and R. F. Kramer, *Nat. Biotechnol.* **1998**, *16*, 49-53.
3. Kostrikis, L. G., S. Tyagi, M. M. Mhlanga, D. D. Ho, and F. R. Kramer, *Science* **1998**, *279*, 1228-1229.
4. Whitcombe, D., J. Theaker, S. P. Guy, T. Brown, and S. Little, *Nat. Biotechnol.* **1999**, *17*, 804-807.
5. Thelwell, N., S. Millington, A. Solinas, J. Booth, and T. Brown, *Nucl. Acids Res.* **2000**, *28*, 3752-3761.
6. Jenkins, Y. and J. K. Barton, *J. Am. Chem. Soc.* **1992**, *114*, 8736-8738.
7. Svanvik, N., G. Westman, D. Wang, and M. Kubista, *Anal. Biochem.* **2000**, *281*, 26-35.
8. Carreon, J. R., K. P. Mahon, Jr., and S. O. Kelley, *Org. Lett.* **2004**, *6*, 517-519.
9. Dervan, P. B. and B. S. Edelson, *Curr. Opin. Stuct. Biol.* **2003**, *13*, 283-299.
10. Rucker, V. C., S. Foister, C. Melander, and P. B. Dervan, *J. Am. Chem. Soc.* **2003**, *125*, 1195-1202.
11. Fechter, E. J. and P. B. Dervan, *J. Am. Chem. Soc.* **2003**, *125*, 8476-8485.
12. Fechter, E. J., B. Olenyuk, and P. B. Dervan, *Angew. Chem. Int. Ed.* **2004**, *43*, 3591-3594.
13. Lee, L. G., C. H. Chen, and L. A. Chiu, *Cytometry* **1986**, *7*, 508-517.
14. Rye, H. S., M. A. Quesada, K. Peck, R. A. Mathies, and A. N. Glazer, *Nucl. Acids Res.* **1991**, *19*, 327-333.
15. Nygren, J., N. Svanvik, and M. Kubista, *Biopolymers*, **1998**, *46*, 39-51.

16. Rye, H. S., S. Yue, D. E. Wemmer, M. A. Quesada, R. P. Haugland, R. A. Mathies, and A. N. Glazer, *Nucl. Acids Res.* **1992**, *20*, 2803-2812.

17. Benson, S. C., P. Singh, and A. N. Glazer, *Nucl. Acids Res.* **1993**, *21*, 5727-5735.

18. Spielmann, H. P., D. E. Wemmer, and J. P. Jacobsen, *Biochemistry* **1995**, *34*, 8542-8553.

19. Baird, E. E. and P. B. Dervan, *J. Am. Chem. Soc.* **1996**, *118*, 6141-6146.

20. Trauger, J. W. and P. B. Dervan, *Methods Enzymol.* **2001**, *340*, 450-466.

21. Swalley, S. E., E. E. Baird, and P. B. Dervan, *J. Am. Chem. Soc.* **1997**, *119*, 6953-6961.

22. Swalley, S. E., E. E. Baird, and P. B. Dervan, *J. Am. Chem. Soc.* **1996**, *118*, 8198-8206.

23. Dickinson, L. A., R. J. Gulizia, J. W. Trauger, E. E. Baird, D. E. Moiser, J. M. Gottesfeld, and P. B. Dervan, *Proc. Natl. Acad. Sci. USA* **1998**, *95*, 12890-12895.

24. Zeman, S. M. and D. M. Crothers, *Methods Enzymol.* **2001**, *340*, 51-68.

25. Zeman, S. M., K. M. Depew, S. J. Danishefsky, and D. M. Crothers, *Proc. Natl. Acad. Sci. USA* **1998**, *95*, 4327-4332.

26. Bondensgaard, K. and J. P. Jacobsen, *Bioconj. Chem.* **1999**, *10*, 735-744.

27. Staerk, D., A. A. Hamed, E. B. Pedersen, and J. P. Jacobsen, *Bioconj. Chem.* **1997**, *8*, 869-877.

28. Svanvik, N., J. Nygren, G. Westman, and M. Kubista, *J. Am. Chem. Soc.* **2001**, *123*, 803-809.

29. Best, T. P., B. S. Edelson, N. G. Nickols, and P. B. Dervan, *Proc. Natl. Acad. Sci. USA* **2003**, 100, 12063.

30. Edelson, B. S., T. P. Best, B. Olenyuk, N. G. Nickols, R. Doss, S. Foister, A. Heckel, and P. B. Dervan, *Nucl. Acids Res.* **2004**, 32, 2802.

31. Brooker, L. G. S., G. H. Keyes, and W. W. Williams, *J. Am. Chem. Soc.* **1942**, *64*, 199-210.

32. Kim, Y.-S., K. M. Kim, R. Song, M. J. Jun, and Y. S. Sohn, *J. Inorg. Biochem.* **2001**, *87*, 157-163.

33. Maxam, A. M. and W. S. Gilbert, *Methods Enzymol.* **1980**, *65*, 499-560.

34. Iverson, B. L. and P. B. Dervan, *Methods Enzymol.* **1996**, *15*, 7823-7830.